Structural Nonlinearity Extraction from Video Data for Damage Evaluation in Earthquake Events: Experimental Verification

SIFAN WANG and MAYUKO NISHIO

ABSTRACT

A development of a method of structural nonlinearity extraction is introduced for fast evaluation of structural damage conditions in post-earthquake events using the video data that is taken and shared in societies. The video data-based structural analysis has advanced rapidly in recent years due to advantages of non-contact data acquisitions, high spatial resolution in low-cost device, and so on. This study presents the experimental verification conducted by the shaking table tests, and to extract singularities spatial domains due to nonlinearity events using computer vision (CV)-based technology. In the shaking table test, two three-story aluminum frame models, whose modal frequencies are designed to become slightly different, are used to introduce some kinds of structural nonlinearities, such as hitting, boundary condition changes, and residual deformations in some of members. The present study solely concentrates on boundary condition nonlinearity, which is achieved by incorporating a controllable hinge member with a trigger magnet at the base of the columns to simulate the boundary constraint change from fixed end to hinge end during excitation. When the input excitation level is large enough, the magnets detach and cause the boundary constraint to change. A video camera is put in front of the model to capture the whole experiment, and the acquired video data are used for the verification. Optical flow method, as an effective video processing technique, can be used to estimate the real-world object motion between observer and scene by a dense field corresponding to the interframe displacement of each pixel. Farneback optical flow algorithm is selected here to extract the motion information of models; Then, the node strength index is introduced as the feature extraction to detect the nonlinearity events. The change in boundary conditions can significantly alter structural local motion information, leading to a clear mutation in node strength that can serve as an indicator of nonlinearity events. The results in this experimental study show the possibilities of video-based technology for the fast damage condition evaluation in the post-earthquake.

Sifan Wang, Department of Engineering Mechanics and Energy, University of Tsukuba, 1-1-1 Tennodai, Tsukuba, Ibaraki Prefecture, 305-0006, Japan

INTRODUCTION

Recently, modern sensing technologies have been used by structural health monitoring (SHM) to detect damage and assess civil-infrastructure performance. The availability of key structural response data is essential for SHM investigations and engineering applications [1]. In general, the traditional data-driven structural response monitoring approach is used for such purposes. However, this approach becomes less beneficial due to some practical limitations, including the inconsistency of reference location for displacement response measurement, the incompatible behavior between the global structural response and the locally installed attached sensors, incomplete data observation due to limited instrumentation, and temporary interruption in the data acquisition process due to system maintenance are among few of them [2-3]. To cope with these limitations, different methods such as wireless sensors, Kalman-filter-based response estimators, Global Positioning System (GPS), and, particularly, Computer-vision (CV) based methods have been employed for the efficiency improvement and capacity enhancement of the SHM-system applicability [4].

Recently, CV-based methods are becoming more popular in the field of SHM owing to their potential characteristics like cost efficiency, non-contact full-field measurements capability, and ease of operation [5]. With the advancement in CV, cameras have been extensively used as contactless sensors for SHM. The acquisition of video data has also become easier, which makes video-based structural damage evaluation methods more promising.

During the progression of structural damage, a multitude of nonlinearity events are likely to arise. Although such nonlinearity events may not be indicative of damage alone, they can serve as a key indicator of suspected damage, rendering the detection of such nonlinear events an effective approach for detecting structural damage occurrences. The manifestation of nonlinearity events in structural vibration is most prominently expressed through the motion characteristics of the structure. As such, observing the motion of the structure is a viable approach for identifying structural nonlinearity events. Optical flow, as an effective video processing technique, can be used to estimate the real-world object motion between observer and scene by a dense field corresponding to the interframe displacement of each pixel. The implementation of the optical flow method is based on a series of assumptions, and the assumptions vary for different optical flow methods. For instance, the Lucas-Kanade (LK) localized optical flow method is applied to the laboratory experiment by assuming the brightness consistency and small displacement about the tracking point [6]. The more advanced Farneback optical flow method employs a binary quadratic polynomial for the brightness intensity function for the neighborhood area in the region of interest (ROI), which enables full-field motion estimation and more complicated trajectory tracking [7]. The extraction of motion information lays the foundation for the nonlinearity events evaluation of the structure. Subsequently, the localization of structural damages can be achieved by integrating the relevant feature extraction indicators.

Moreover, shake table test has emerged as a prominent technique for conducting structural dynamic and damage evaluation during seismic events. The test has the capability to accurately replicate the failure modes and damage patterns of actual structures under earthquake conditions. It is often utilized to assess both linear or nonlinear, elastic or inelastic dynamic responses of structures. Furthermore, the strategic placement of video cameras enables the gathering of detailed footage containing pertinent damage information.

This paper presents a novel approach for localizing nonlinearity events by designing a shake table test to simulate a strong nonlinear event: boundary constraint changes during excitation (boundary-condition nonlinearity). Additionally, the node strength network feature index based on Farneback optical flow is employed to localize the nonlinearity events using video data. Initially, a dynamic response test is performed to determine the resonance frequencies of the two models, which enables an understanding of the structure's state and aids in selecting an appropriate frame rate for subsequent video capture. Subsequently, the Farneback optical flow algorithm is utilized to calculate the optical flow. A repulsive force-weighted network is then constructed, and the node strength matrix is obtained by utilizing the node degree as the characteristic parameter. Finally, the normalized node strength matrix is leveraged to detect structural nonlinearity during earthquake events.

METHODOLOGY

The Farneback optical flow and node strength network are employed for structural motion estimation and nonlinearity extraction. The video data is collected and pre-processed at first. Then, the proposed methods are used to extract the nonlinearity features and localize the damages. For both methods, a detailed mathematical formulation and framework are presented in the following sub-sections.

Farneback Optical Flow Method

Optical flow, as an effective video processing technique to analyze displacement of objects, can be generally categorized into two types: sparse optical flow and dense optical flow. The sparse optical flow only needs to process local pixels from the whole image, e.g., the Lucas-Kanade method (LK). In contrast, the dense optical process of all the pixel points of an image is time-consuming but can be more accurate, e.g., the Horn-Schunck method (HS) and the Farneback method. Here, the Farneback method uses a polynomial expansion, which allows it to model more complex motion patterns than the linear models used by HS and LK algorithms. As a result, the Farneback algorithm can estimate the motion of objects with more complicated trajectories.

For the Farneback optical flow method, the basic assumption is that in a small image neighborhood area, the brightness intensity function $f(x, y)$ of the pixel vector $p = (x\ y)^{\mathrm{T}}$ can be approximately expressed by a binary quadratic polynomial:

$$f(x, y) \sim a_0 + a_1 x + a_2 y + a_3 x^2 + a_4 y^2 + a_5 xy \tag{1}$$

Eq. (1) can be written in matrix form as follow:

$$f(p) \sim p^{\mathrm{T}}\mathbf{A}p + b^{\mathrm{T}}p + \mathrm{c} \tag{2}$$

where **A** is a symmetric matrix, b is a vector, and c is a scalar, respectively,

$$\mathbf{A} = \begin{bmatrix} a_3 & \frac{a_5}{2} \\ \frac{a_5}{2} & a_4 \end{bmatrix} \quad \mathrm{b} = \begin{pmatrix} a_1 \\ a_2 \end{pmatrix} \quad \mathrm{c} = a_0 \tag{3}$$

In order to solve this Eq. (2), the exact quadratic polynomial at time t is considered as:

$$f_t(p) = p^{\mathrm{T}}\mathbf{A}_t p + b_t^{\mathrm{T}} p + \mathrm{c}_t \tag{4}$$

After a short time interval Δt, the displacement of p is Δp $(\Delta x, \Delta y)$, so the brightness intensity of $(p + \Delta p)$ at a time $(t + \Delta t)$ is:

$$f_{t+\Delta t}(p + \Delta p) = (p + \Delta p)^{\mathrm{T}}\mathbf{A}_{t+\Delta t}(p + \Delta p) + b_{t+\Delta t}^{\mathrm{T}}(p + \Delta p) + \mathrm{c}_{t+\Delta t} \tag{5}$$

Expanding the Eq. (5), it follows:

$$f_{t+\Delta t}(p + \Delta p) = p^{\mathrm{T}}\mathbf{A}_{t+\Delta t}p + (b_{t+\Delta t} + 2\mathbf{A}_{t+\Delta t}\Delta p)^{\mathrm{T}}p + \Delta p^{\mathrm{T}}\mathbf{A}_{t+\Delta t}\Delta p + b_{t+\Delta t}^{\mathrm{T}}\Delta p + \mathrm{c}_{t+\Delta t} \tag{6}$$

And then, if $\mathbf{A}_t$ is not singular, the global displacement Δp between two consecutive images I_1 and I_2 can be obtained as follows:

$$\Delta p = -1/2\ \mathbf{A}_{t+\Delta t}{}^{-1}\,(b_{t+\Delta t} - b_t)\Delta p = -1/2\ \mathbf{A}^{-1}_{t+\Delta t}\,(b_{t+\Delta t} - b_{\mathrm{t}}) \tag{7}$$

So the motion information can be estimated pointwise according to Eq. (7). To reduce the influence of noise, the error function e of the neighborhood area N can be constructed:

$$e = \sum_{\Delta N \in N} \omega\,(\Delta N)\|\mathbf{A}(p + \Delta N)\Delta p - \Delta b(p + \Delta N)\|^2 \tag{8}$$

where $\omega(\Delta N)$ is the Gaussian weighting function in neighborhood area N and $\Delta b = -1/2\ (\mathrm{b}_{t+\Delta t} - \mathrm{b}_t)$. In this study, a 9 by 9 pixel neighborhood area is selected, considering the calculation time and identification accuracy. The weighting function can reflect the influence degree of each point in the neighborhood area and the value will increase as each pixel is close to the target pixel in the neighborhood area.

Node Strength Network

Following the occurrence of nonlinearity events, such as sudden boundary changes, the structure frequently experiences sudden changes in the velocity vector (magnitude and orientation) of the local area during earthquake events. These velocity changes can be utilized to construct a network of all pixel points in the image data, where the interaction force between two nodes is represented as an edge in the network. The presence of an edge between the nodes is determined by the repulsive force between the nodes, with the inertial centrifugal force F being chosen to reflect the repulsive force. When a nonlinearity event occurs in a region and causes an increase in repulsive force towards adjacent regions, the boundaries can be detected. For a given field, the inertial centrifugal force between the central pixel point (x_0, y_0) and other points in a two-dimensional neighborhood N of size ($x_0 \pm \varepsilon$, $y_0 \pm \varepsilon$) can be expressed by the following formula [8-9]:

$$\vec{F}_{ij} = -m_i k_{ij} \frac{v_{ij}^2}{d_{ij}} \vec{e}_{ij} \tag{9}$$

where m_i is the mass of the pixel point i. All the mass of points are set as unit 1 in this paper. d_{ij} is the distance between point i and point j and the unit is pixel, $\vec{e}_{ij}$ is the orientation vector. v_{ij} and k_{ij} is the relative velocity and a coefficient that can be determined by the following equation, respectively:

$$v_{ij} = \begin{cases} (\vec{v}_i - \vec{v}_j)\cdot\vec{e}_{ij}, & \text{if } (\vec{v}_i - \vec{v}_j)\cdot\vec{e}_{ij} > 0 \\ 0, & \text{otherwise} \end{cases} \tag{10}$$

$$k_{ij} = \begin{cases} (\vec{v}_i \cdot \vec{e}_{ij}) / \|\vec{v}_i\|, & \text{if } \vec{v}_i \cdot \vec{e}_{ij} > 0,\ v_i \neq 0 \\ 0, & \text{otherwise} \end{cases} \tag{11}$$

Then, for the adjacency matrix, the node strength $s(i)$ of node i can be constructed and expressed as follow:

$$\mathrm{s}(i) = \sum_{n=1}^{j} \left|\vec{F}_{ij}\right| \tag{12}$$

After calculating each pixel point of the image, the node strength matrix $\mathbf{S}$ of a grayscale image containing c columns and r rows can be obtained:

$$\mathbf{S} = \begin{bmatrix} s_{11} & \cdots & s_{1\mathrm{c}} \\ \vdots & \ddots & \vdots \\ s_{\mathrm{r}1} & \cdots & s_{\mathrm{rc}} \end{bmatrix} \tag{13}$$

DESCRIPTIONS OF THE TEST MODEL

In this study, a three-story aluminum frame model with a controllable hinge bearing is used in a shake table test to simulate changes in structural boundary conditions. The dimensions of the column are 630 mm (length), 30 mm (width), and 2 mm (height), while the plate is a square with a side length of 200 mm and a thickness of 10 mm. The first three order resonance frequencies of the model using fixed end are 6.82 Hz, 19.2 Hz, and 28.37 Hz. The overall model is depicted in Figure 1, while Figure 2 shows the design of the controllable hinge bearing used to simulate the changes in boundary conditions. Initially, the magnet is connected to the iron block and the connection is fixed. However, upon input of seismic waves, the magnet will detach, resulting in a change in the boundary condition from a fixed connection to a hinge connection. Such changes in boundary conditions can alter the vibration

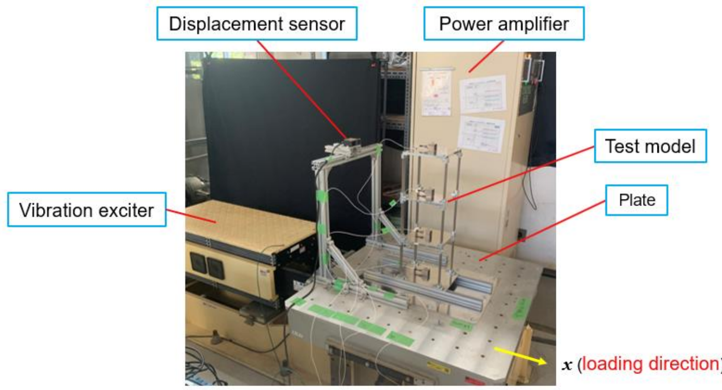

Figure 1. Overall diagram of test model.

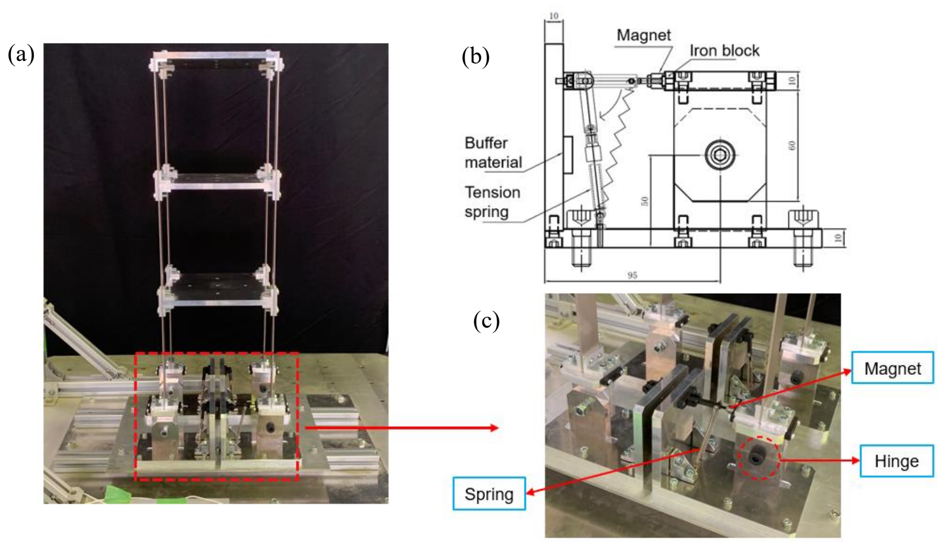

Figure 2. (a) Test model with hinge bearing (b) Size drawing (c) Details of bearing.

mode (the displacement d_x and the rotation r_x change to free) of the structure and give rise to strong nonlinearity in the system. In addition, a random signal with a frequency range of 3-50 Hz and a root mean square (RMS) acceleration of 0.1 standard gravity is selected as the input wave, generated using MATLAB. The video data is acquired using a Sony FDR-AX700 camera with a pixel resolution of 1920×1080 and a frame rate set to 120 fps to comply with the Nyquist sampling theorem, which requires the sampling frequency to be greater than twice the maximum resonance frequency of the models. Due to insufficient indoor lighting, two lamps are used to provide supplemental lighting during the video capture process to reduce excessive noise in the video.

IDENTIFICATION RESULTS

To accurately determine the change in vibration pattern of the model following the boundary condition change and the precise time of the change, an accelerometer

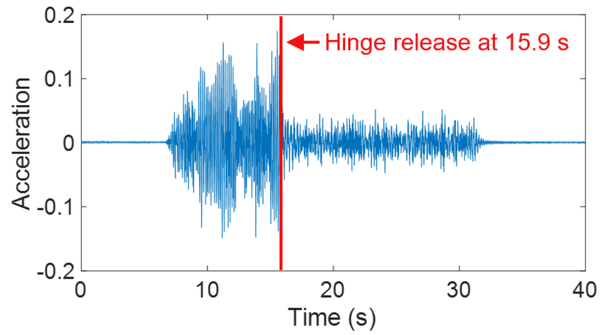

Figure 3. Acceleration response of the top floor.

is strategically placed on the top floor of the model. This enabled the precise measurement of acceleration changes both before and after the boundary condition change, and the result is presented in Figure 3. The acceleration response at the top floor of the model shows a significant change at approximately 16 seconds (see Figure 3), indicating that the boundary condition of the model has changed at this time. The observed change in the acceleration response can be attributed to the energy dissipation caused by the hinge bearing.

The following step is the acquisition and analysis of video data. To capture the entire process, a 1-minute video is recorded, which includes the 25.6 seconds of the input wave. To improve computational efficiency, only 2-second segments that contain pounding events are extracted and processed at a lower resolution. Using Farneback optical flow, the velocity and orientation of all pixel points are computed for each frame. Based on this information, a node strength network is constructed. The results of the three phases (before, during, and after the change) are presented in Figure 4. It can be seen that during the boundary changes, the bearing regions exhibit dense highlight parts (as seen in the yellow rectangle area), and the motion pattern of the base floor changes as well (as evidenced by the disappearance of the highlight part in Figure 4(b) compared with Figures 4(a) and 4(c)). These observations suggest that nonlinearities exist in this region during this process.

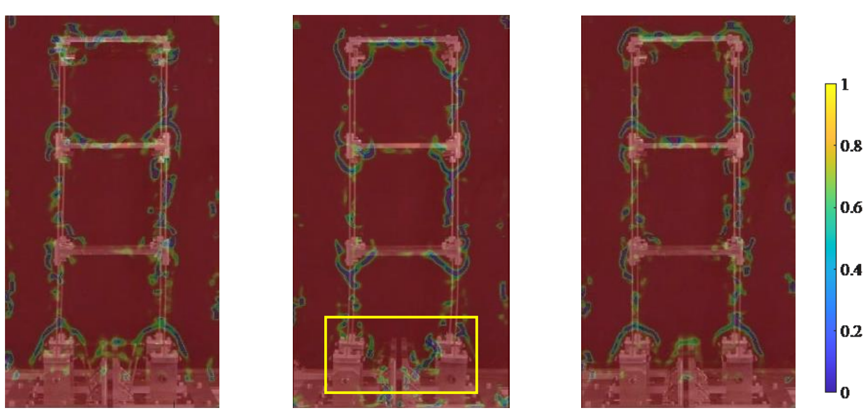

(a) t = 15.5 s (b) t = 15.9 s (c) t = 17 s

Figure 4. The visualization results of the three phases: (a) before (b) during and (c) after the boundary condition changes.

CONCLUSIONS

This study aims to develop a methodology to identify and localize nonlinearity events during boundary condition changes using shake table tests with a frame structural model. The proposed method employs the Farneback optical flow algorithm and the repulsive force model to extract and characterize the nonlinearity. First, the video sequence frames are processed by the Farneback optical flow algorithm to obtain the velocity vector field. Second, the repulsive force network between two pixel nodes is determined using a certain condition. The strength of each node in the network is used to construct a two-dimensional feature matrix. Finally, the nonlinearity events are visualized and localized based on this matrix. The results demonstrate that the proposed method can successfully identify the nonlinearity events during the boundary condition change process. However, the presence of other highlight parts (background and the edge of each floor of the model) reduces the identification accuracy. In future work, the second-order difference method is explored to address this issue. In addition, the time at which the nonlinearity event occurs is also crucial information regarding the extent of the damage. Therefore, the identification of singularity time will also be investigated. Finally, real-world disaster video data of structures will be analyzed to verify the effectiveness of the proposed method.

ACKNOWLEDGMENT

This work was supported by JST SPRING (Grant number JPMJSP2124).

REFERENCES

1. Strauss, A., J. Bien, H. Neuner and C. Harmening. 2020. "Sensing and monitoring in tunnels testing and monitoring methods for the assessment of tunnels," *Structural Concrete*, 21(4): 1356-1376,
2. Baqersad, J., P. Poozesh, C. Niezrecki, and P. Avitabile. 2017. "Photogrammetry and optical methods in structural dynamics – A review," *Mech Syst Signal Process*, 86: 17-34.
3. Oh, B. K., J. W. Hwang, Y. Kim, T. Cho, and H. S. Park. 2015. "Vision-based system identification technique for building structures using a motion capture system," *J Sound Vib*, 356: 72-85.
4. Dong, C. Z., and F. N. Catbas. (2021). A review of computer vision–based structural health monitoring at local and global levels. *Struct Health Monit*, 20(2): 692-743.
5. Yang, Y., C. Dorn, T. Mancini, Z. Talken, G. Kenyon, C. Farrar., and D. Mascareñas. 2017. Blind identification of full-field vibration modes from video measurements with phase-based video motion magnification. *Mech Syst Signal Process*, 85: 567-590.
6. Lucas, B. D., and T. Kanade. 1981. An iterative image registration technique with an application to stereo vision. In *IJCAI'81: 7th international joint conference on Artificial intelligence*, 2: 674-679.
7. Farnebäck, G. 2003. Two-frame motion estimation based on polynomial expansion. In *Image Analysis: 13th Scandinavian Conference, SCIA 2003 Halmstad, Sweden*, 13: 363-370.
8. Zhang, X., D. Lin, J. Zheng, X. Tang, Y. Fang and H. Yu. 2019. Detection of salient crowd motion based on repulsive force network and direction entropy. *Entropy*, 21(6), 608.
9. Chraibi, M., A. Seyfried, and A. Schadschneider. 2010. Generalized centrifugal-force model for pedestrian dynamics. *Physical Review E*, 82(4), 046111.